getech

Coastal Upwelling

User Guide

Getech, Kitson House, Elmete Hall, Elmete Lane, Leeds LS8 2LJ, UK
Getech Inc., 3000 Wilcrest Dr. Suite 155, Houston, TX 77042, USA
UK. +44 113 322 2200 USA. +1 713 979 9900 info@getech.com www.getech.com

Table of Contents

1. Introduction

Coastal upwelling occurs when Ekman transport (i.e. where wind-driven currents diverted by the Coriolis effect cause the net movement of ocean surface water at right angles to the wind) takes place away from the coast. As the surface water moves away from the coast, it is replaced by nutrient-rich bottom water. Areas of coastal upwelling are typically characterised by high productivity and are associated with the deposition of organic-rich sediments.

The importance of high primary productivity associated with upwelling as a factor in the origin and distribution of organic-rich marine sediments has been recognised since at least the 1930s (Trask, 1934). Not only did coastal upwelling become one of the key modern analogues for source rock deposition during the 1980s, its predictable relationship to wind patterns and the Coriolis force means that it also became the primary palaeoclimatological-palaeogeographic approach to large scale modelling of marine source rock distribution (e.g. Barron, 1985; Barron & Moore, 1994; Kruijs & Barron, 1990; Miller, 1989; Moore et al., 1993, 1995; Parrish, 1982, 1995; Parrish & Curtis, 1982; Scotese & Summerhayes, 1986). The primary focus of this effort has been the coastal upwelling associated with the major Eastern Boundary Upwelling Systems (EBUS), as seen in the modern California Current, Humboldt Current (Peru-Chile), Canary Current (northwest Africa) and Benguela Current (Namibia), plus monsoon-related upwelling, as seen in the modern Arabian Sea. These areas appear to be the ones most associated with the SiPC association in the fossil record (i.e. sediments enriched in biogenic silica, phosphorus and organic carbon). There has been less focus on upwelling linked to equatorial divergence as this process is not linked to coastlines; instead, it occurs mostly over deep oceanic waters, and its relevance to effective ancient source rocks (i.e. those likely to reach maturity and whose generated hydrocarbons are likely to encounter accessible potential reservoirs) has yet to be clearly demonstrated.

For coastal upwelling to occur at all, there are two essential oceanographic conditions that must be present (Figure 1):

- Vertical upward movement of stratified nutrient-rich bottom water into the mixed ocean layer (MOL); this results in nutrient-rich bottom water being brought into the photic zone.

- Horizontal movement of the surface water in an offshore direction; this draws mixed surface water away from the coast and redeposits the organic matter in stratified water offshore.

Furthermore, these two essential conditions must coexist during the same part of the year; if they do not, then coastal upwelling will not occur. For example, if one of the conditions existed from January to June and the other condition only existed from July to December, an annual average of these conditions would show moderate values for coastal upwelling; however, this would actually be a false result as no coastal upwelling would occur at all if there was no cross-over between the two essential conditions being in place at the same time of the year. Therefore, it is crucial to assess where these conditions exist on monthly basis.

Two additional oceanographic conditions also need to be considered as they have a direct impact on coastal upwelling and can restrict it: latitudinal light limitation (as upwelling without light will not be expressed in palaeoproductivity) and sea ice coverage (as sea ice will both inhibit light penetration and reduce the depth of the photic zone).

Owing to the seasonal nature of coastal upwelling signals, Getech's initial Coastal Upwelling Model produced monthly data layers for each of the four variables that favour coastal upwelling conditions, generating 48 Globe data layers per timeslice. The results allowed the user to assess the conditions for each month. However, the results from the initial model did not provide users with a succinct and easy metric with which they could quickly and easily gauge the location, intensity and persistence of coastal upwelling.

Significant improvements to Getech's Coastal Upwelling Model have been made since its initial launch in 2014. In the present iteration, we have attempted to utilise several of the general circulation model (GCM) outputs in an integrated fashion, along with using filters that help to constrain the spatial pattern of coastal upwelling. The latest developments have enabled Getech to re-evaluate the palaeoclimate ocean data and thus 1) define areas of coastal upwelling more effectively and 2) summarise the data as integrated annual maps that show both the persistence and the intensity of coastal upwelling conditions. These summary maps are included in the Globe 2019 delivery for all 58 timeslices in Globe.

The aim of this user guide is to show the user how modelled palaeo-oceanographic data have been used to predict where potential areas of coastal upwelling were located in the past. This user guide will outline the technical theory used to create Getech's Coastal Upwelling Model, describe the model principals and the methodology used, and give examples of the data that the model produces.

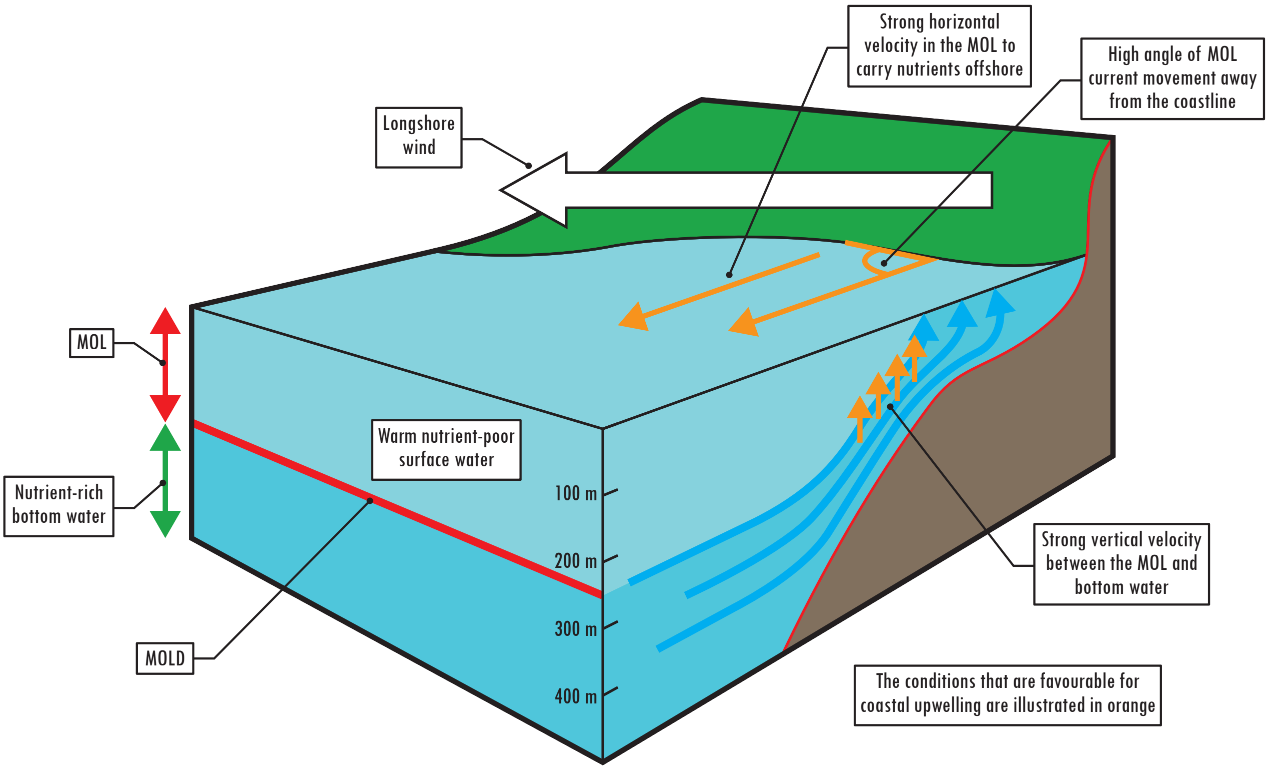

Figure 1: The key oceanographic conditions required for effective coastal upwelling to take place.

2. The Modelling Principals Used to Define the Coastal Upwelling Signal

The four key oceanographic conditions that provide the best potential for coastal upwelling to occur are as follows:

1. The vertical upward movement of stratified water across the MOL: This is critical as it supplies stratified nutrient-rich bottom water to the photic zone, allowing organic matter to be produced in this zone.

2. An offshore current: The movement of the surface water in an offshore direction is important as it draws mixed surface water away from the coast and redeposits the organic matter in stratified water offshore.

3. Daylight length of 8 hours or more per day: This amount of light is enough to allow photosynthesis to occur in phytoplankton.

4. Less than 50% sea ice cover: Sea ice cover of 50% or less does not restrict light penetration into the photic zone; therefore, photosynthesis in phytoplankton is not inhibited by this level of sea ice cover.

The width of the upwelling-influenced zone in classic modern coastal upwelling areas (e.g. the areas affected by the Benguela, Canary, Humboldt and California Currents) varies spatially and temporally and can extend up to 300 km offshore (e.g. Hagen et al., 2001). Within this zone, the upwelling signal will decrease with distance offshore ('downstream'), as the frequency of events that extend beyond a given distance decreases (although those events that extend furthest will be more intense). The mixed layer nutrients become progressively depleted by plankton growth with time and downstream distance, and the impacts on the sediment record will be diminished by any increase in water depths that would result in decreased carbon delivery fluxes. It is therefore necessary to apply a spatial mask as this lets us focus our upwelling predictions more specifically on coastal or shelf-break zones.

Based on the above observations, the original Coastal Upwelling Model employed a uniform 250 km wide zone that extended offshore from the coastline, but we have since modified our approach. This is because in the case of palaeogeographic configurations with wide shallow shelves that are too shallow to be stratified, the locus of upwelling will be displaced offshore to the shelf/slope boundary, which may lie more than 250 km from the coastline, and thus would be excluded from consideration if a fixed distance of 250 km was used. We have thus utilised a 'pseudo-coastline' based upon the boundary between stratified and mixed waters (i.e. where the depth becomes deeper than the ocean mixed layer (MOLDcor). This boundary will vary seasonally and with bottom gradient, the width of the potential upwelling zone being defined by its spatial range, the offshore limit where the depth is always >MOLD, and the onshore limit where it is always <MOLD (i.e. during all 12 months). At any one time (month), the upwelling front will be located along the landward edge of the stratified zone, but with its influence extending offshore. This is undoubtedly a simplification but is probably a realistic one given the 0.5° spatial resolution of the GCM. Lateral variation within the zone of potential upwelling is not explicitly taken into account, other than that produced by the lateral annual migrations of the edge of the stratified zone.

There are several important caveats to this approach of modelling potential source rocks:

- Not all source rocks are products of upwelling or of upwelling alone; most are probably not.
- There remain significant methodological uncertainties with regard to the robustness of reported levels of agreement between predicted upwelling and source rock occurrence that is potentially explicable by upwelling (i.e. the type of statistic used, exactly how it is calculated and its genuine significance).
- Upwelling is a widespread phenomenon that occurs at a wide range of spatial scales, intensities, frequencies and persistence; therefore, generalisations should be treated with caution.
- Upwelling addresses only the supply of nutrients by Ekman divergence (although it is made more relevant to phytoplankton productivity by also considering the availability of light); consequently, not all upwelling results in the production of organic-rich (or oil-prone) sediments due to the influence of other regional or local factors (e.g. water depth, oxygen levels, current strengths, sediment grain size, siliciclastic dilution and biogenic autodilution).
    - Onshore aridity and areas of low fluvial discharge are factors that can be used in conjunction with predicted upwelling to help define areas of favourably low dilution by siliciclastic sediment.
- Any organic-rich sediment produced is not necessarily permanently preserved (e.g. due to subsequent erosion or reworking of the outer shelf and upper slope), and it may also not acquire an adequate thickness.

3. Methods

For modelling purposes, it is assumed that modelled palaeo-oceanographic data from Globe's Earth system model (ESM) can be used to depict the oceanographic conditions that define coastal upwelling; therefore, the data can also be used to indicate the locations of areas that had potentially high ocean productivity throughout geological history.

The model defines areas of potential coastal upwelling during any given month as being:

- In water deep enough to be stratified
- Within 250 km of the frontal zone
- Where there is a net upward movement of water across the base of the OML
- Where there is a net offshore movement of the surface water (relative to the local coastline generalised at a 0.5° level)
- Where daylight length is not limiting (i.e. at least 8 hours of daylight per day)
- Where sea ice cover is limited to less than 50%

The conditions listed above are combined to show the spatial distribution of the occurrence of upwelling conditions, but the combination will not give a sense of the intensity of its signal. To obtain a measure of the intensity of the coastal upwelling signal, the strength of both the offshore current and the vertical upward movement of the ocean must be assessed. The greater the velocity of these currents, the greater the influx of nutrients into the photic zone and the greater the volume of organic matter carried away from the coastal ocean mixed zone, resulting in an increased likelihood of organic matter being deposited.

The model produces three annual summary layers of coastal upwelling frequency/intensity per timeslice:

1. Upwelling annual frequency: Showing only the number of months upwelling exists regardless of its intensity.

2. Upwelling annual average intensity: Showing an upwelling index that integrates the vertical and horizontal velocities, the transport direction and the available light for all 12 months.

3. Average intensity of upwelling months: Showing the annual intensity index values averaged over the number of months an upwelling signal is present.

The following sub-sections show how Globe's palaeo-oceanographic and palaeogeographic data have been combined to produce the annual frequency and intensity data. The sub-sections also 1) describe how each of the six key upwelling conditions listed above are defined using Globe's palaeo-oceanographic data, 2) depict the necessary workflows undertaken by the model to depict each of the key upwelling conditions, and 3) outline how the key upwelling conditions are combined spatially and temporally to produce annual and monthly summary maps.

3.1 Methods for Determining the Key Upwelling Conditions From Existing Globe Data

All of the Globe ESM data used in the modelling process are monthly. As a first step, it is critical to assess the monthly data to determine 1) spatially where the upwelling conditions required existed in a given month and 2) the strength of that upwelling signal. This accomplishes two things: 1) it preserves information on the seasonality of the signal that can then be assessed at a later stage in the modelling process, and 2) it eliminates any data values being included in annual summaries where the conditions for upwelling were not all met. The following sub-sections describe the processes applied by the model to determine the spatial extent of the upwelling conditions defined for each month. Once the monthly data have been analysed, they can be combined to produce annual summaries.

3.1.1 Determining the frontal zone and the 250 km area of upwelling

Data required:

- Globe palaeobathymetry layers
- Globe ESM palaeoclimate monthly mixed ocean layer depths (MOLDs)

Here, the frontal zone is defined as the area where the MOLD intersects with the bathymetry (Figure 2). Water shallower than this point will be completely mixed and will not have any stratified nutrient-rich bottom water to bring to the surface. As the MOLD varies by month, the point of intersection with the bathymetry will also vary by month; it is therefore essential to assess the frontal zone and 250 km area of upwelling on a monthly basis.

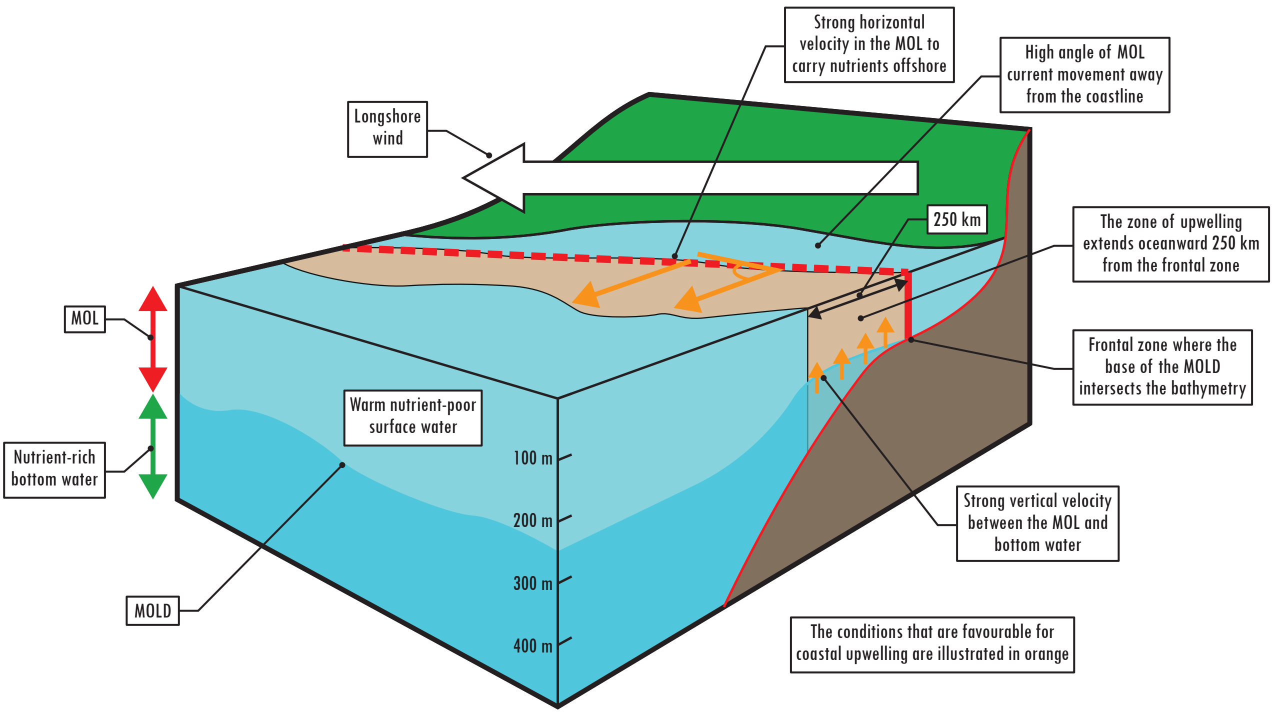

Figure 2: Box diagram showing how the frontal zone and the 250 km area of upwelling are defined.

Once the frontal zone line is determined, it is then possible to generate a 250 km buffer from this line that extends in a seaward direction; this buffer will define the 250 km zone of coastal upwelling for each month. Any data positioned outside this zone will be masked out as they are considered beyond the offshore extent of upwelling (based on Present Day observations). The workflow outlined in Figure 3 shows the necessary steps taken to determine the frontal zone and the 250 km area of upwelling.

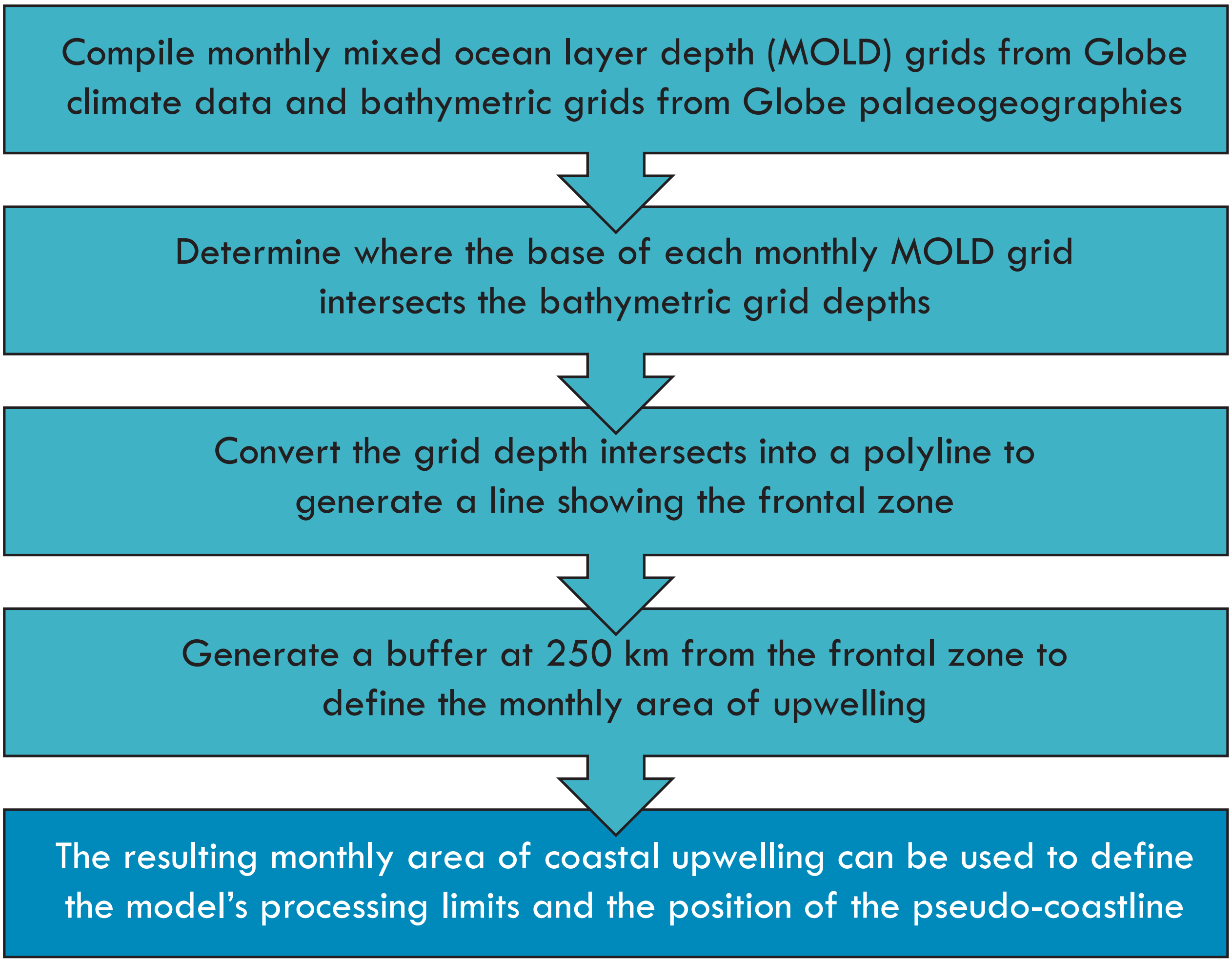

Figure 3: *Workflow for determining the frontal zone and the 250 km area of upwelling.*

3.1.2 Determining if stratified waters are brought into the ocean mixed layer

Data required:

- Globe ESM palaeoclimate monthly MOLDs
- Globe ESM palaeoclimate monthly ocean vertical velocity depth layers
- Monthly area of coastal upwelling (calculated in previous step)

The next stage in the modelling process is to determine if there is vertical upward movement of nutrient-rich stratified ocean waters into the MOL. This can be done using the monthly MOLDs (as they represent the boundary between the stratified deeper ocean water and the oxygenated mixed layer) and the vertical velocity data (as these data show the net vertical movement of water in the ocean). The model isolates the relevant vertical velocity grid values for all depth layers that intersect with the MOLD (Figure 4); this generates a single grid with the velocity values at the MOLD.

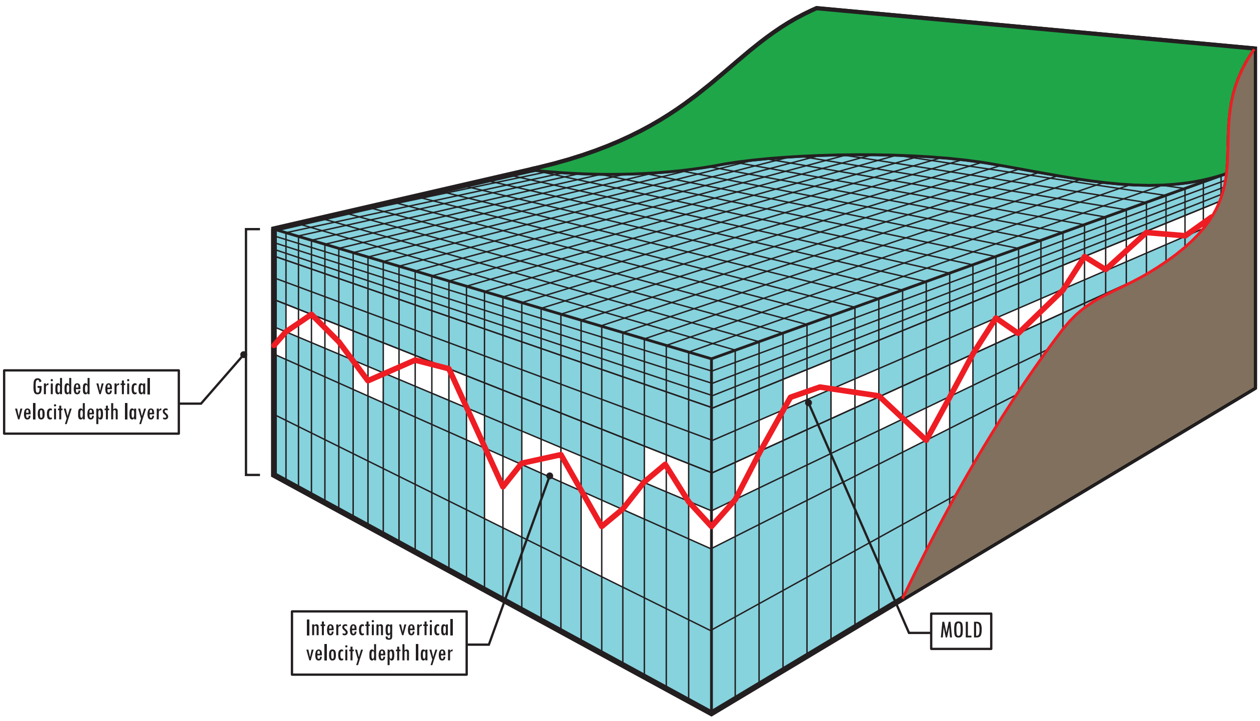

Figure 4: Schematic box diagram showing how the model intersects the mixed ocean layer depth (MOLD) with different vertical velocity depth grids.

The velocity values are positive for the upward movement of water and negative for the downward movement of water; as upwelling requires the upward movement of water, the model filters out any negative values, leaving only the velocity values for upward moving water. The data are then masked against the monthly extent of upwelling determined by the 250 km masks described in the previous sub-section.

The workflow used for this part of the modelling is shown in Figure 5. The final layer from this process shows the spatial extent of vertical upward movement through the MOL boundary; this layer is used in the modelling for both the monthly and annual summaries.

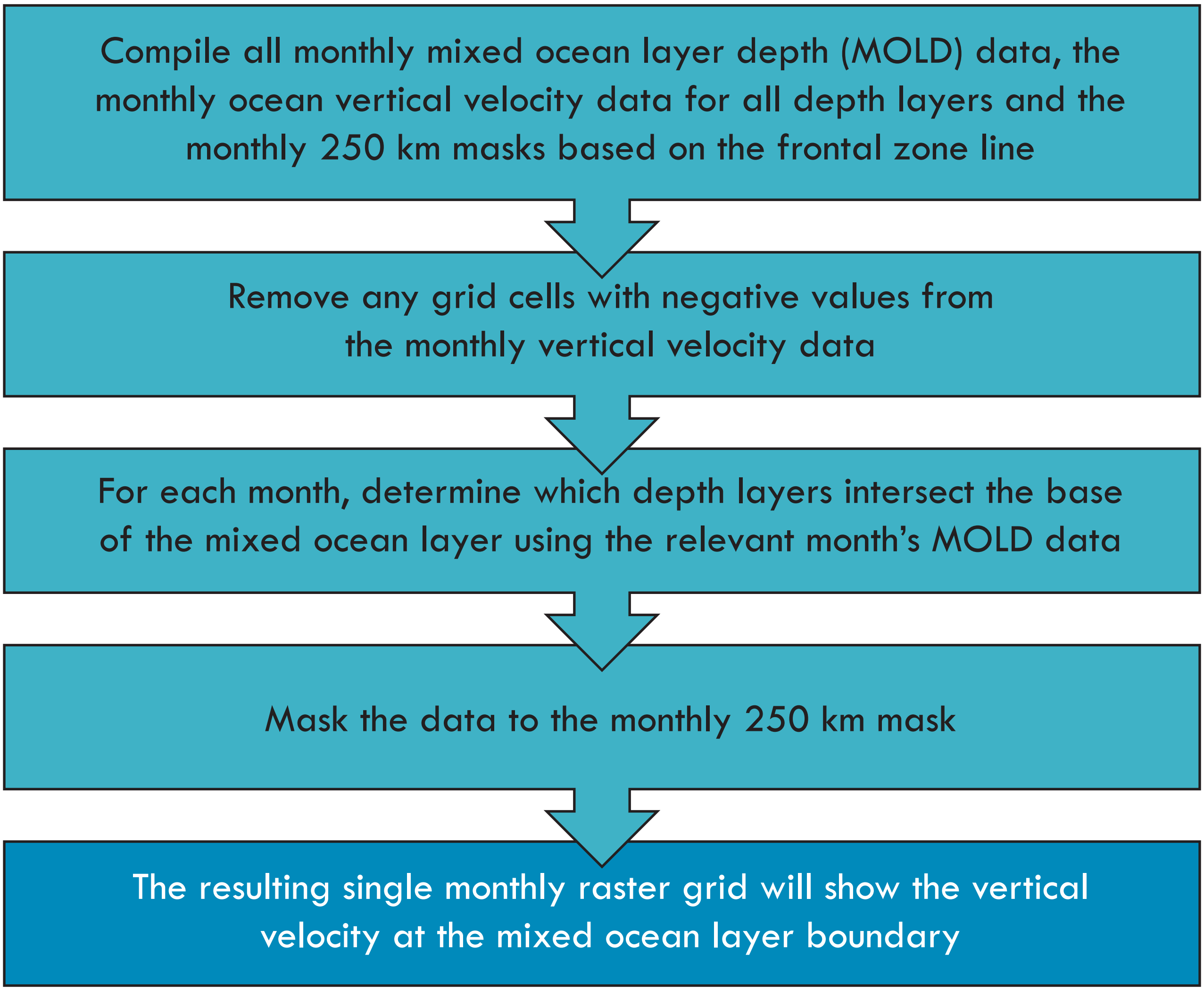

Figure 5: *Workflow for determining the vertical velocity at the mixed ocean layer boundary.*

3.1.3 Determining if there is an offshore current in the surface water

Data required:

- Frontal zone polylines (calculated in a previous step)
- Monthly zone of coastal upwelling (calculated in a previous step)
- Globe ESM palaeoclimate monthly ocean horizontal velocity depth layers

It is essential to establish if the nutrient-rich waters that were brought to the surface at a specified point in time were carried offshore away from the frontal zone. If these waters were driven from the frontal zone in an onshore direction, then there will have been no stratified bottom water available for the organic matter produced to have been deposited and preserved within the sediment. Any organic matter that remained in the shallow mixed oxygenated water is likely to have been oxidised and not preserved in the sediments deposited. Therefore, the model considers the frontal zone to be a pseudo-coastline, and the 'offshore' current is calculated relative to this instead of the coastline (Figure 2).

In order to determine if an offshore current existed at a certain point in time, a number of steps must be taken (Figure 6). Initially, the frontal zone polyline (acting as a pseudo-coastline) is generalised to 0.5 degrees; this converts the polyline into a series of straight lines from which its orientation relative to north can be calculated.

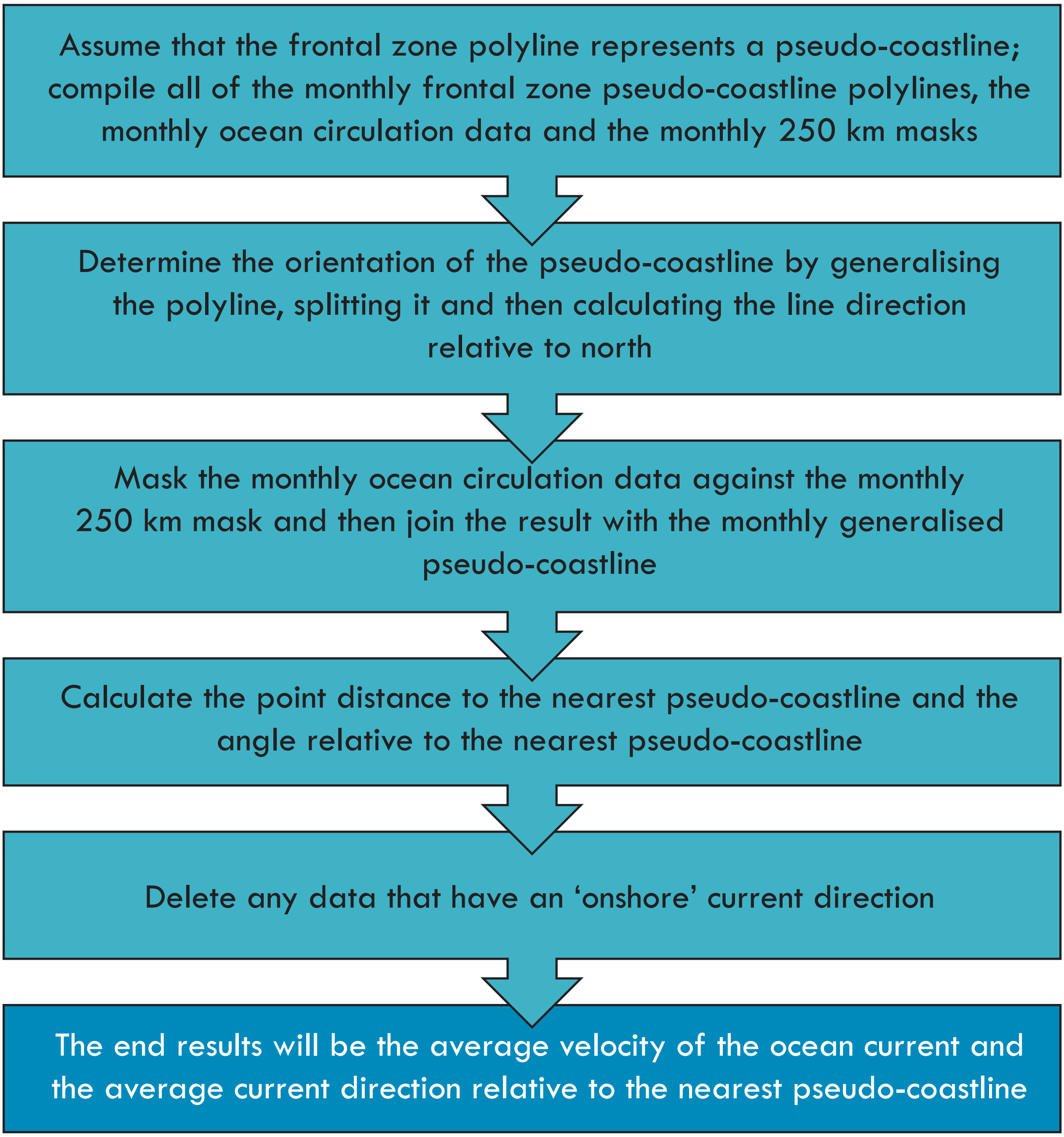

Figure 6: Workflow to determine if an offshore current exists relative to the pseudo-coastline.

The next step in the modelling process is to establish the direction of the current in the surface water. The surface water in this model encompasses the upper five depth layers of the ocean circulation data. These depth layers correspond to the upper 50 m of the water column and are considered the most significant ones as this where the majority of photosynthesis takes place. These data are masked to the relevant monthly 250 km area of upwelling (determined in a previous step in Section 3.1.1). The data are then joined to the nearest section of the monthly pseudo-coastline, based on the point distance to the pseudo-coastline.

Once the data have been joined to the pseudo-coastline, the angle relative to the pseudo-coastline can be calculated. The data are then filtered to leave only the offshore current values (i.e. values between 0 and 90 relative to the pseudo-coastline). These values are then averaged through the five surface depth layers to generate a single point data set with the average offshore current direction and velocity in the surface water. These data values are exported to produce two separate raster grids, with one showing the average current direction relative to the pseudo-coastline and the other showing the average velocity of the current. These raster grids will be used in the modelling for both monthly and annual summaries.

3.1.4 Filtering for daylight length limitations and sea ice cover

As upwelling can only influence productivity where and when light is available, the mean monthly daylight length variation with latitude and season is used to determine whether daylight is likely to be limiting or not for the month(s) of predicted upwelling. The objective is to help identify the likely distribution of effective (non-light-limited) upwelling productivity.

The mean monthly length of daylight is calculated from the formula of Forsythe et al. (1995), which corrects for latitude and the Julian day of the year (seasonality) for both hemispheres (arbitrary fifteenth day of the month values are used for monthly calculations). Present Day orbital parameters are assumed. Spatial filtering of the predicted coastal upwelling is applied according to a minimum required daylight length of 8 hours for plankton blooming, based upon Ardyna et al. (2013) for the modern Arctic Ocean. At least some of the upwelled nutrients that cannot be utilised at the time of physical upwelling because of low light levels (or too deep a MOLD) may be utilised later in the year, boosting productivity once light improves and the MOLD is reduced. However, the nutrient-rich cold water may sink or be exported. No such effects are included in the model.

The GCM estimated sea ice coverage ('concentration') is also used as a spatial filter to further constrain the distribution of productivity-effective upwelling. High latitude productivity is likely to be positively correlated with the proportion of open water (Ardyna et al., 2014). In the absence of data, we have assumed a maximum permissible sea ice concentration of 0.5 (i.e. 50% of a grid cell).

The productivity of upwelling zones will be greatest where the MOLD is less than the thickness of the euphotic zone. Under such circumstances the phytoplankton are never light-limited. When the mixed layer is deeper (as happens in winter), mixing will carry the phytoplankton below the euphotic zone for part of the time, limiting the primary productivity. Of course, during winter the euphotic zone will also be shallower (especially at higher latitudes) and daylight length will be shorter. At the moment, we have not yet included the euphotic depth in our model, although generalised algorithms are available that could be utilised for this purpose. Its inclusion would further constrain productivity-effective upwelling to the spring to autumn period (i.e. not winter) and would amplify latitudinal gradients.

To summarise, both seasonal daylight length and sea ice have limiting effects on photosynthesis. For modelling purposes, it is assumed that photosynthesis becomes limited if an area receives less than 8 hours of daylight per day and if it has over 50% sea ice cover. These parameters roughly correspond with the limits of high-latitude productivity blooms. Daylight length is determined by latitude and the time of year, while sea ice cover is derived directly from the climate model. Any data that either do not meet the required minimum number of daylight hours or exceed the sea ice cover limits are removed by the model.

3.2 Generating Monthly and Annual Summary Layers

3.2.1 Upwelling annual frequency summary layer

Once the model has determined where each of the coastal upwelling conditions existed on a monthly basis, it is possible to stack these monthly conditions to determine the spatial extent of areas where all of the requirements for an upwelling signal were met each month.

These 12 monthly frequency layers can be combined to show the number of months the upwelling signal was present for each year (Figure 7). This is the first annual summary layer provided to users and it is named ‘upwelling annual frequency’; it consists of a grid that shows values ranging from 1 to 12, with the numbers representing the number of months in a year that the upwelling signal was present, irrelevant of its intensity.

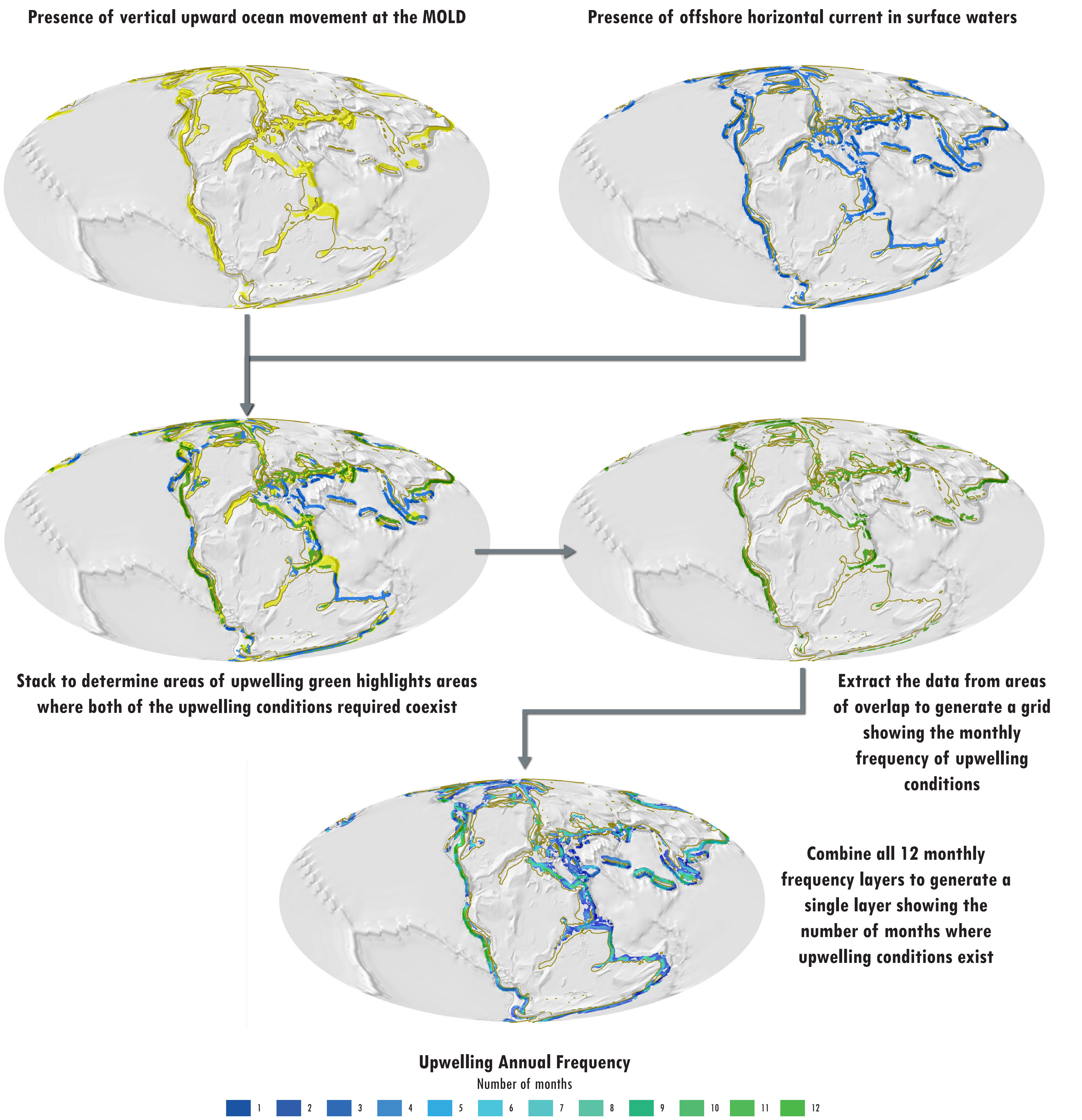

Figure 7: *Workflow for determining the number of months where upwelling conditions existed to produce an upwelling annual frequency data layer.*

3.2.2 Upwelling monthly intensity summary layer

The monthly summaries for the vertical velocity at the MOLD, the offshore current velocity and the surface ocean current direction relative to the nearest pseudo-coastline all contain velocity/vector values within the data. These values can be used to generate a sense of the monthly intensity of the upwelling signal.

To evenly weight the values of the data, they are converted into a percentage of the maximum value. This brings all the data values for each of the three conditions down to a value of between 0 and 100. Once they are filtered by the various masks (i.e. the 250 km extent of upwelling, sea ice and daylight filters), the resulting intensity grids can be stacked and combined to show a monthly intensity of the coastal upwelling signal; the resulting data layer is called 'upwelling monthly intensity' (Figure 8). The model will only combine values where all three conditions exist. This layer allows the user to assess the strength of the coastal upwelling signal on a monthly basis.

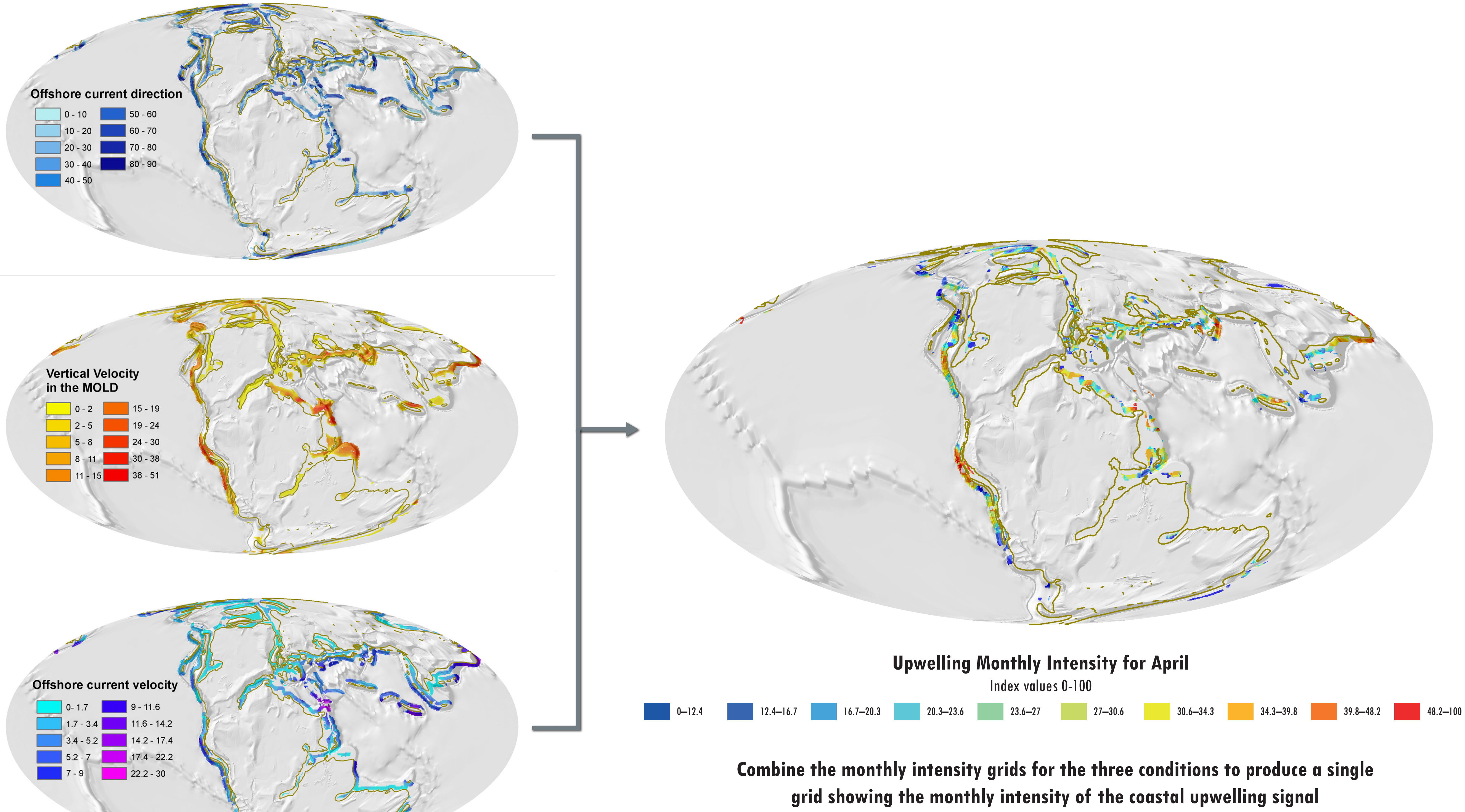

Figure 8: *Workflow used to produce an upwelling monthly intensity data layer.*

3.2.3 Upwelling annual average intensity layer and average intensity of upwelling months layer

Once the monthly intensity values of all the upwelling conditions have been combined, it is then possible to summarise them as an annual average. This has been achieved in a simple way by summing the values of the 12 monthly layers and then dividing the total by 12 to return the intensity values back to a single percentage value that ranges from 0 to 100. The resulting data layer is called 'upwelling annual average intensity'; it gives an overall average of the strength of the coastal upwelling signal throughout the year, but it does not distinguish whether that signal strength/weakness is down to a few months of strong upwelling or down to several months of weak upwelling. This is where the monthly intensity data can become useful.

A further useful summary of these data is provided by taking the annual intensity sum and dividing this by the number of months the upwelling signal existed. The resulting data layer is called 'average intensity of upwelling months'; it shows the average intensity for the months of the year where the upwelling conditions actually existed, rather than being averaged over the entire year. This will give a more informed metric for the strength of the upwelling signal when it existed, without the need to search through all 12 monthly summaries.

3.3 Overview of the Modelling Processes

Figure 9 provides a summary workflow of the modelling methods applied by Getech's Coastal Upwelling Model. In particular, the workflow outlines the input data used in the modelling, the simplified steps applied in the modelling processes and the output summary data generated.

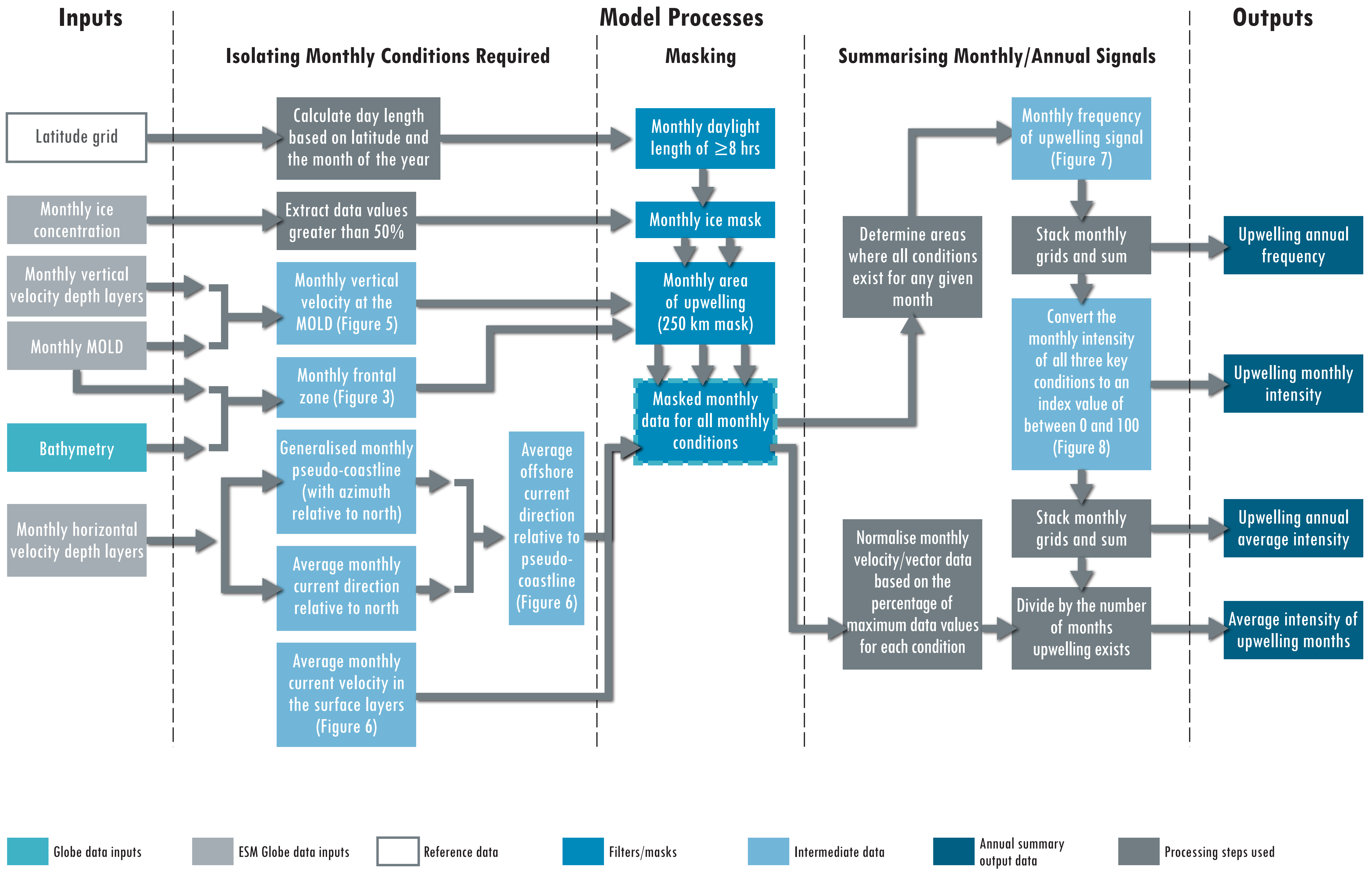

Figure 9: Summary workflow of the modelling methods applied by Getech's Coastal Upwelling Model.

4. Summary of the Data Delivered

The new modelling methods applied by Getech's Coastal Upwelling Model have allowed us to 1) re-evaluate the palaeo-oceanographical data to better define areas of coastal upwelling and 2) summarise the data in integrated annual/monthly layers; these layers are described in the following sub-sections. The layers show both the frequency and intensity of the coastal upwelling signal for each of the 58 timeslices in Globe. When used in tandem, these layers form a basis upon which users can estimate the possible distribution of upwelling-related phenomena through time and then compare these distribution estimates with actual observations.

We have taken the coastal upwelling frequency and intensity maps produced for the modern day palaeogeography (using the same methodologies as have been used for the ancient palaeogeographies) and visually compared them with modern maps of phytoplankton productivity. It should be noted that the magnitudes of upwelling and productivity are not directly correlatable on a global scale (even when light is taken into account) because the nature (e.g. nutrient concentration) and age of the upwelled water varies, and there are often additional factors (such as turbidity). However, the maps do show a reasonable correspondence with the modern zones of high productivity, especially the classic EBUS, whose ranked magnitude is also correct (Humboldt = Benguela > California > Canary).

4.1 Upwelling Annual Frequency Layers

The upwelling annual frequency data layers provide an annual summary of the total number of months in a year for which upwelling conditions (of any magnitude) existed in each grid cell within the zone of potential non-light-limited upwelling. The upwelling condition is defined by the presence of any positive (upward) vertical velocity in the depth layer containing the base of the MOL, plus the presence of any lateral horizontal velocity in a direction that is offshore relative to the averaged orientation of the boundary between stratified and mixed waters (pseudo-coastline). These data layers provide the user with a sense of the persistence of the coastal upwelling signal throughout a specified year. The data do not consider the strength of that signal, only its temporal pattern. An example of the data layers provided in Globe is shown in Figure 10.

4.2 Upwelling Monthly and Annual Intensity Layers

Three conditions were used to measure upwelling intensity: 1) the monthly vertical velocities at the depth that intersects the base of the MOLD, 2) the monthly horizontal velocities in the surface water layers (i.e. the upper 55 m) and 3) the monthly angles (0–90°) between the direction of the horizontal movement and the generalised pseudo-coastline. Each of these three parameters was calculated as a percentage relative to the sum of their maximum observed values so that they could be combined (despite their different units and scales) to produce a single overall percentage value that could be plotted on one map as either a monthly summary or an annual summary.

4.2.1 Average intensity of upwelling months layers

These data layers show the sum of the monthly upwelling intensity divided by the number of months where an upwelling signal existed. This provides the user with a sense of the strength of the upwelling signal when it existed, instead of it being smoothed out over the year. When these data are used in conjunction with the upwelling annual average intensity data, users are able to determine whether the intensity values are a result of a strong/weak seasonal signal or a persistent signal. An example of the data layers provided in Globe is shown in Figure 11.

4.2.2 Upwelling annual average intensity layers

This set of data layers shows the sum of the monthly upwelling intensity data divided by 12 to give an average annual summary of the strength of the upwelling signal smoothed over the year. These data layers help the user to gain an insight into the relative annual strength of the signal, but they do not distinguish whether the strength/weakness of the signal is due to the strength of the signal or its persistence. An example of the data layers provided in Globe is shown in Figure 12.

4.2.3 Upwelling monthly intensity layers

These data layers summarise the strength of the coastal upwelling signal for each month of the year to show the intensity of upwelling for each month. The data displayed will only show intensity values for months where all upwelling conditions were present; thus, there can be variation in the spatial distribution of data for each month of the year. An example of the data layers provided in Globe is shown in Figure 13.

4.3 Symbology

All summary data (excluding the upwelling annual frequency layers) are symbolised into 10 categories based on each tenth centile of the data distribution of Present Day data sets for that particular data set. This is considered the best way to display the variation within the data sets and it best represents the variation present in the majority of the data values. The individual data values are preserved in the grid, and different symbologies can be applied to best suit the user's individual needs if required.

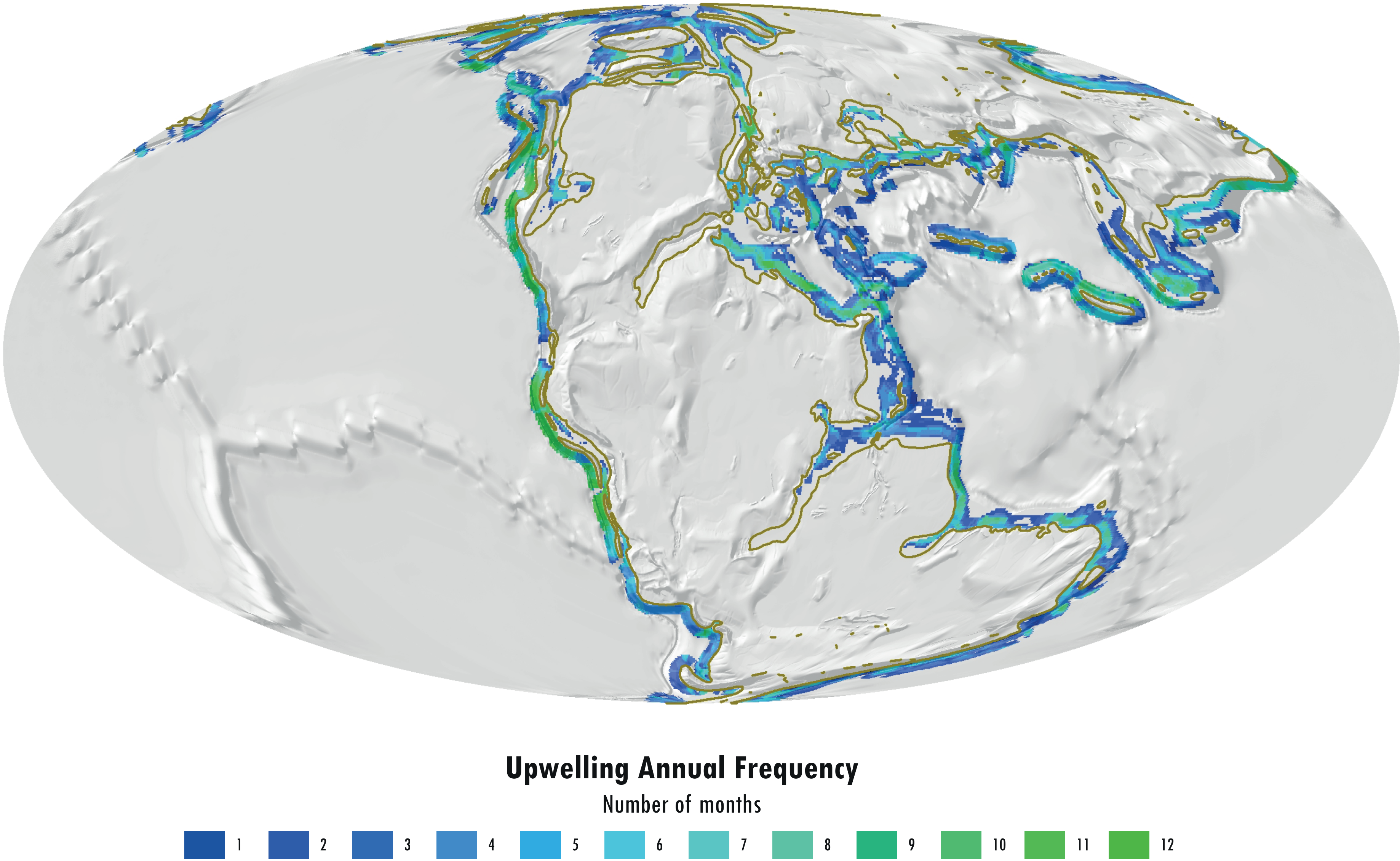

Figure 10: *An example of an upwelling annual frequency layer for the Bajocian, showing the number of months in the year in which upwelling conditions existed.*

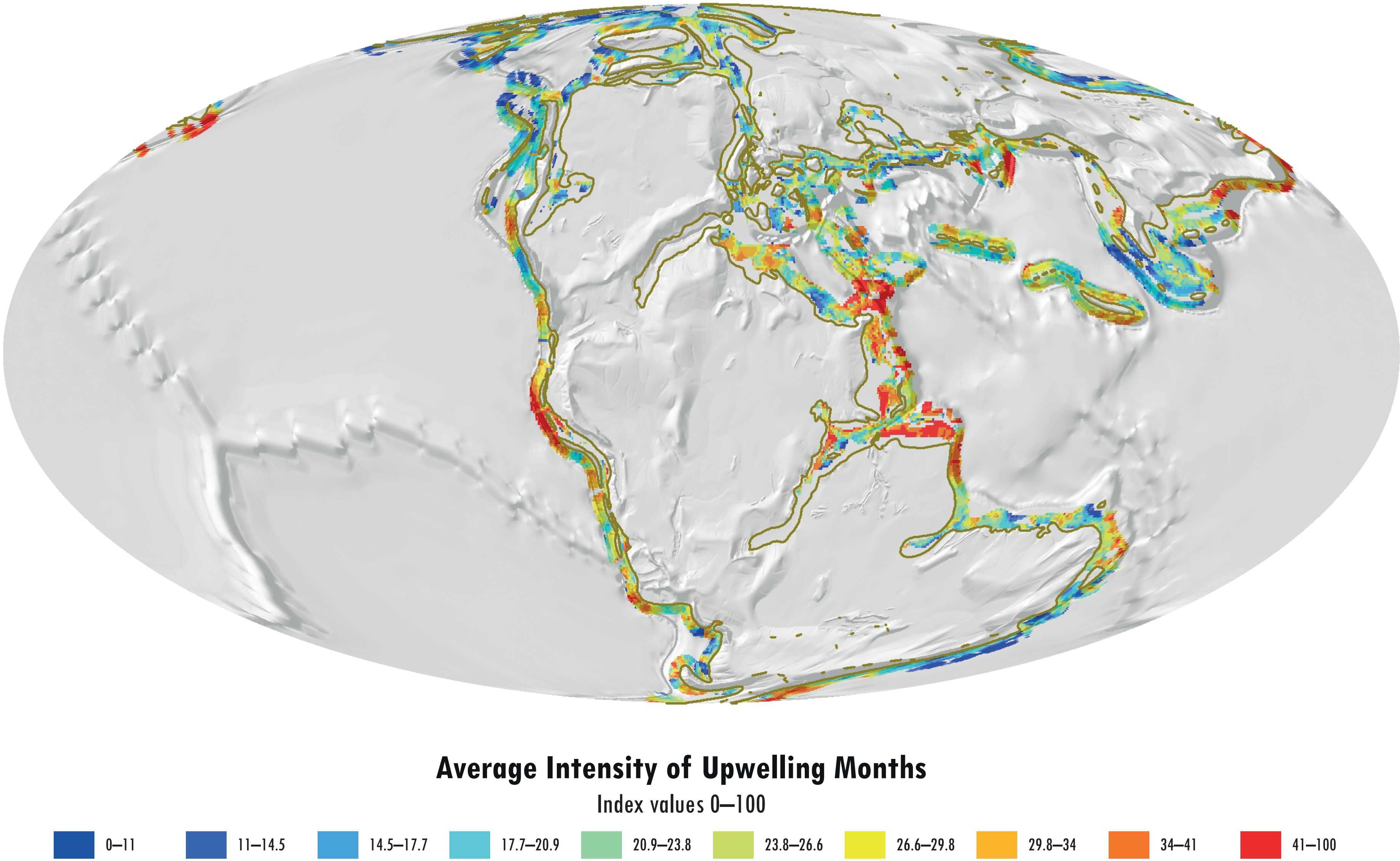

Figure 11: *An example of an upwelling monthly intensity data layer for the Bajocian, showing the total intensity values of all months of upwelling divided by the number of months where upwelling actually occurred.*

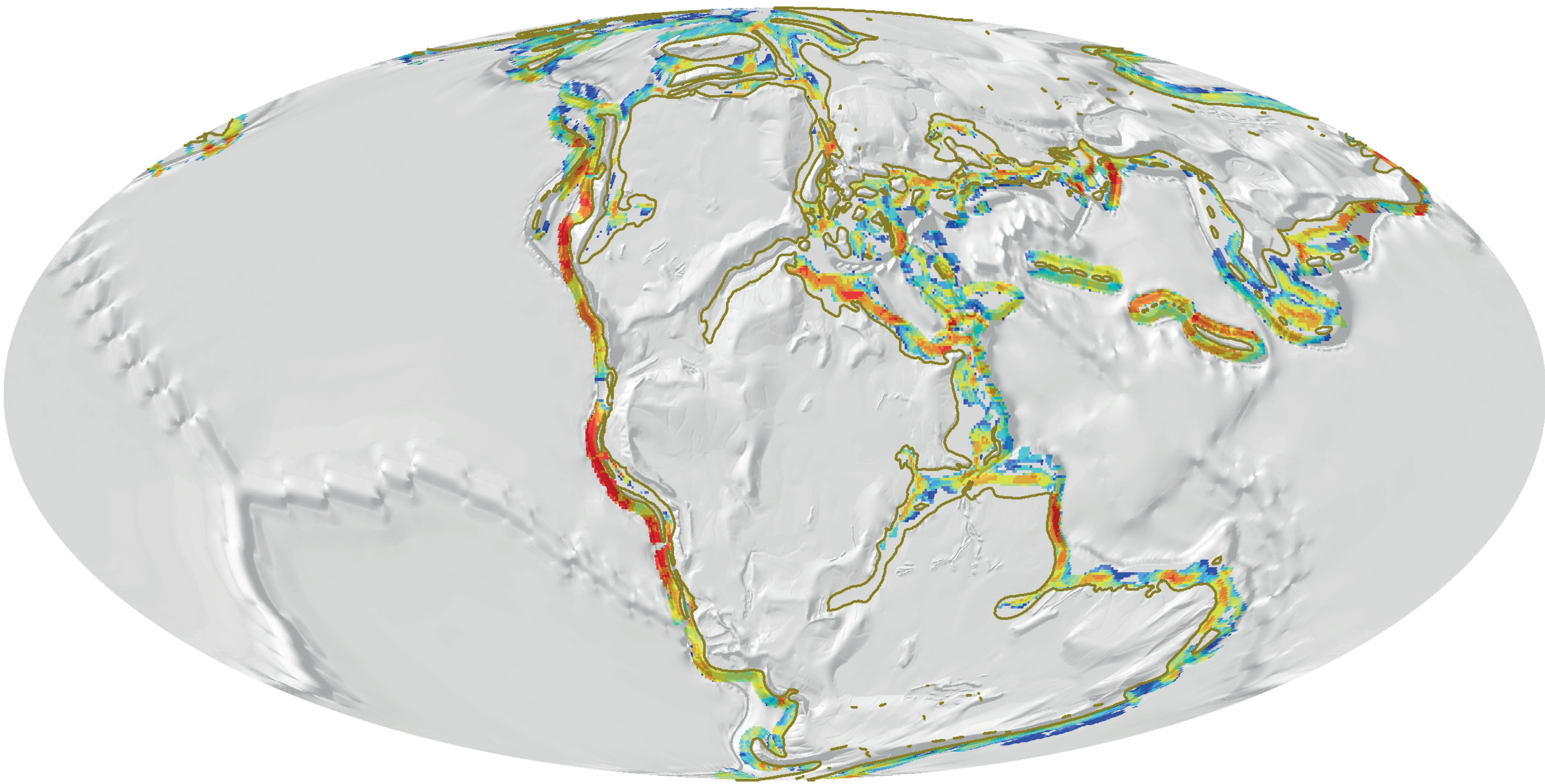

Upwelling Annual Average Intensity

Index values 0–100

0–1.3 | 1.3–2.2 | 2.2–3.4 | 3.4–4.8 | 4.8–6.6 | 6.6–9 | 9–12.6 | 12.6–17.3 | 17.3–24.5 | 24.5–100

Figure 12: *An example of an upwelling annual average intensity data layer for the Bajocian, showing the upwelling intensity values of all months averaged over the year.*

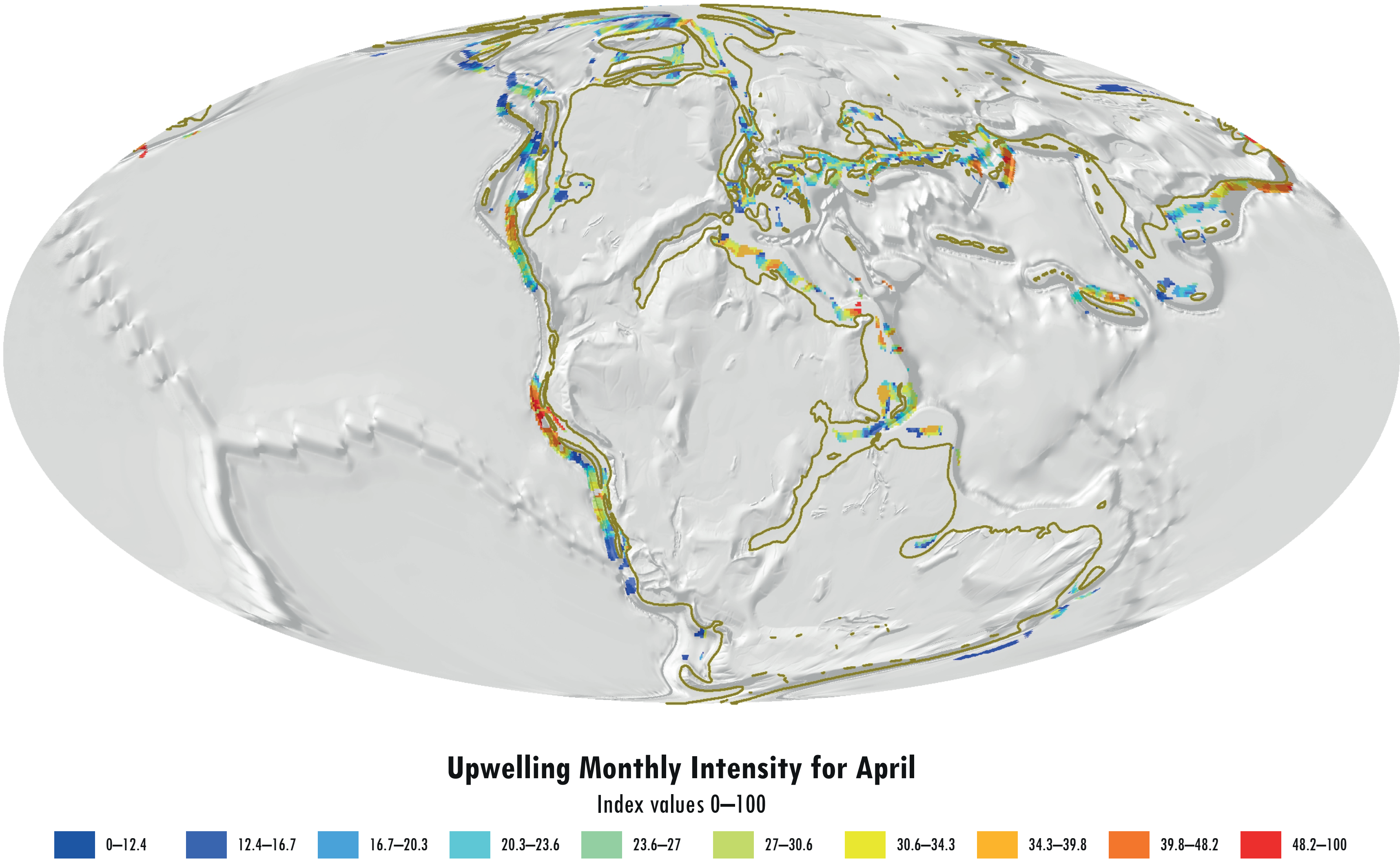

Figure 13: *An example of a Bajocian average intensity of upwelling months data layer for April, showing the average intensity values of all upwelling conditions for the month.*

5. References

Ardyna, M., Babin, M., Gosselin, M., Devred, E., Bélanger, S., Matsuoka A. & Tremblay, J.-É. (2013). Parameterization of vertical chlorophyll a in the Arctic Ocean: impact of the subsurface chlorophyll maximum on regional, seasonal, and annual primary production estimates. *Biogeosciences*, 10 (6), pp. 4383-4404, doi: 10.5194/bg-10-4383-2013.

Ardyna, M., Babin, M., Gosselin, M., Devred, E., Rainville, L. & Tremblay, J.-É. (2014). Recent Arctic Ocean sea ice loss triggers novel fall phytoplankton blooms. *Geophysical Research Letters*, 41 (17), pp. 6207-6212, doi: 10.1002/2014GL061047.

Barron, E. J. (1985). Numerical climate modeling, a frontier in petroleum source rock prediction: results based on Cretaceous simulations. *AAPG Bulletin*, 69 (3), pp. 448-459, doi: 10.1306/ad46250b-16f7-11d7-8645000102c1865d.

Barron, E. J. & Moore G. T. (1994). Upwelling prediction. In: E. J. Barron & G. T. Moore (Eds.) *Climate Model Applications in Paleoenvironmental Analysis*, SEPM Short Course Notes, 33, pp. 109-129, doi: 10.2110/scn.94.03.0109.

Forsythe, W. C., Rykiel, E. J., Stahl, R. S., Wu, H.-I. & Schoolfield, R. M. (1995). A model comparison for daylength as a function of latitude and day of year. *Ecological Modelling*, 80 (1), pp. 87-95, doi: 10.1016/0304-3800(94)00034-F.

Hagen, E., Feistel, R., Agenbag, J. J. & Ohde, T. (2001). Seasonal and interannual changes in intense Benguela upwelling (1982–1999). *Oceanologica Acta*, 24 (6), pp. 557-568, doi: 10.1016/S0399-1784(01)01173-2.

Kruijs, E. & Barron, E. J. (1990). Climate model prediction of paleoproductivity and potential source-rock distribution. In: A.-Y. Huc (Ed.) *Deposition of organic facies*, AAPG Studies in Geology, pp. 195-216, doi: 10.1306/St30517C13.

Miller, R. G. (1989). Prediction of ancient coastal upwelling and related source rocks from palaeo-atmospheric pressure maps. *Marine and Petroleum Geology*, 6 (3), pp. 277-283, doi: 10.1016/0264-8172(89)90007-x.

Moore, G. T., Barron, E. J., Bice, K. L. & Hayashida, D. N. (1995). Paleoclimatic controls on Neocomian-Barremian (Early Cretaceous) lithostratigraphy in northern Gondwana's rift lakes interpreted from a general circulation model simulation. In: A.-Y. Huc (Ed.) *Paleogeography, Paleoclimate, and Source Rocks*, AAPG Studies in Geology, 40, pp. 173-189, doi: 10.1306/St40595C8.

Moore, G. T., Hayashida, D. N. & Ross, C. A. (1993). Late Early Silurian (Wenlockian) general circulation model-generated upwelling, graptolitic black shales, and organic-rich source rocks - an accident of plate tectonics? *Geology*, 21 (1), pp. 17-20, doi: 10.1130/0091-7613(1993)021<0017.

Parrish, J. T. (1982). Upwelling and petroleum source beds, with reference to Paleozoic. *AAPG Bulletin*, 66 (6), pp. 750-774, doi: 10.1306/03b5a30e-16d1-11d7-8645000102c1865d.

Parrish, J. T. (1995). Paleogeography of Corg-rich rocks and the preservation versus production controversy. In: A.-Y. Huc (Ed.) *Paleogeography, paleoclimate, and source rocks*, AAPG Studies in Geology, 40, pp. 1-20, doi: 10.1306/St40595C1.

Parrish, J. T. & Curtis, R. L. (1982). Atmospheric circulation, upwelling, and organic-rich rocks in the Mesozoic and Cenozoic eras. *Palaeogeography, Palaeoclimatology, Palaeoecology*, 40 (1-3), pp. 31-66, doi: 10.1016/0031-0182(82)90084-0.

Scotese, C. R. & Summerhayes, C. P. (1986). Computer model of paleoclimate predicts coastal upwelling in the Mesozoic and Cenozoic. *Geobyte*, 1 (3), pp. 28-42.

Trask, P. D. (1934). Deposition of organic matter in recent sediments. In: W. E. Wrather & F. H. Lahee (Eds.) *Problems of Petroleum Geology*, AAPG Special Publication, 6, pp. 27-33, doi: 10.1306/SV6334C3.